Improved Pseudofermion Approach for All-Point Propagators

A. Duncan[1] and E. Eichten[2]

[1]Dept. of Physics and Astronomy, Univ. of Pittsburgh, Pittsburgh, PA 15260

[2]Theory Group, Fermilab, PO Box 500, Batavia, IL 60510

Abstract

Quark propagators with arbitrary sources and sinks can be obtained more efficiently using a pseudofermion method with a mode-shifted action. Mode-shifting solves the problem of critical slowing down (for light quarks) induced by low eigenmodes of the Dirac operator. The method allows the full physical content of every gauge configuration to be extracted, and should be especially helpful for unquenched QCD calculations. The method can be applied for all the conventional quark actions: Wilson, Sheikoleslami-Wohlert, Kogut-Susskind, as well as Ginsparg-Wilson compliant overlap actions. The statistical properties of the method are examined and examples of physical processes under study are presented.

1   Introduction

The development of more powerful computing platforms as well as improvements in algorithms suggest that unquenched lattice QCD gauge configurations on reasonably large lattices should become available in the not too distant future. The generation of equilibrated and decorrelated dynamical gauge configurations for lighter quark masses will nevertheless remain extremely costly in computational terms, and elementary considerations of load-balancing suggest that we should be willing to expend a correspondingly large computational effort in extracting the maximum physical content from each available gauge configuration. Hadronic correlators built from conventional quark propagators (which give the quark propagation amplitude from a single source to all points on the lattice, for example) evidently exploit only a fraction of the physical information latent in each gauge configuration. In this paper we explore the statistical properties and computational feasibility of an alternative stochastic approach to generating quark propagators, one which supplies simultaneously quark propagation amplitudes from any point on a space-time lattice to any other (i.e. all-point propagators). The use of pseudofermion fields has been studied previously [1, 2]; particularly for single light quark systems (e.g. heavy-light mesons). With these approaches, as the quark mass becomes light the convergence of pseudofermion Monte Carlo calculation suffers critical slowing down. In this paper, we observe that for physical correlators (in momentum space) the statistical noise problem resides mainly in its low momentum behaviour. We will find that the convergence can be greatly improved by separating off the lowest eigenmodes of the Dirac operator and treating them exactly while doing the Monte Carlo calculations with a mode-shifted

action.

In Section 2 we review the essential properties of pseudofermion fields which allow the computation of an all-point propagator. Although the detailed results presented in this paper primarily concern Wilson or clover-improved quark actions, we also indicate here how the method can be applied to the computation of an all-point overlap operator. Of course, the basic properties of pseudofermion fields will already be familiar to practitioners of the hybrid MonteCarlo [3] or the Luescher multiboson method [4]. In Section 3 we describe in some detail the use of pseudofermion quark propagators in constructing a variety of hadronic correlators (corresponding to both two- and three-point hadronic Greens functions), such as disconnected parts contributing to form factors or to hairpin amplitudes for isoscalar mesons, etc. In Section 4 we describe the statistical properties of hadronic correlators computed using pseudofermion all point propagators. The availability of all-point propagators allows high-statistics evaluations of the full four-momentum structure of such correlators. Detailed autocorrelation studies reveal that the method gives very accurate results (with rapidly decorrelating amplitudes with a time constant of a few heat-bath sweeps of the pseudofermion fields) for all but the lowest lattice momenta. The critical slowing down in these modes is related to the presence of low eigenmodes of the hermitian Wilson-Dirac operator. Projection and shifting of a few low-lying modes turns out to be computationally straightforward, and finally in Section 5 we show that such mode-shifted pseudofermion simulations allow accurate extraction of *all* momentum components of hadronic correlators.

2 Pseudofermion Actions and All-Point Quark Propagators

A pseudofermion action suitable for computing all-point quark propagators is constructed from the quadratic form Q defining the basic quark action of the theory:

$$S_{\text{quark}} = \sum_{a\mathbf{x},b\mathbf{y}} \bar{\psi}_{a\mathbf{x}} Q_{a\mathbf{x},b\mathbf{y}} \psi_{b\mathbf{y}} \tag{1}$$

where a, b are spin-color indices and $\mathbf{x}, \mathbf{y}$ lattice sites. For the time-being, we shall consider Wilson or clover-improved actions only (later, we return to the case of Ginsparg-Wilson [5] compliant overlap actions). Then the operator $H \equiv \gamma_5 Q$ is hermitian and we can form a positive-definite bosonic ("pseudofermion") action as follows

$$S_{\text{pf}} = \sum_{a\mathbf{x},b\mathbf{y}} \phi_{a\mathbf{x}}^* H_{a\mathbf{x},b\mathbf{y}}^2 \phi_{b\mathbf{y}} \tag{2}$$

in terms of a complex bosonic pseudofermion field ϕ. Averages of products of the pseudofermion field with respect to the Gaussian weight defined in Eq(2) yield inverses of H^2 in the usual way:

$$
\begin{aligned}
<< F(\phi, \phi^*) >> &\equiv Z^{-1} \int d\phi d\phi^* F e^{-S_{\text{pf}}(\phi,\phi^*)} \\
Z &\equiv \int d\phi d\phi^* e^{-S_{\text{pf}}(\phi,\phi^*)} \\
<< \phi_{a\mathbf{x}} \phi_{b\mathbf{y}}^* >> &= \left(H^{-2} \right)_{a\mathbf{x},b\mathbf{y}}
\end{aligned}
\tag{3}
$$

Note that the Gaussian dependence of the pseudofermion action implies

$$<< S_{\text{pf}} >> = N_{\text{col}} N_{\text{spin}} V = 12V \tag{4}$$

where V is the lattice volume (=number of lattice sites). This exact result is extremely useful in checking for errors in the simulation algorithm and in determining equilibration of an ensemble. Of course, the quark propagator of interest in lattice QCD

4

simulations is (up to a trivial γ_5 factor) H^{-1}, not H^{-2}. This can easily be achieved by a single additional "dslash" operation applied to the conjugate pseudofermion field:

$$\tilde{\phi}_{b\mathbf{y}} \equiv (\phi^{\dagger}H)_{b\mathbf{y}}$$

$$<< \phi_{a\mathbf{x}}\tilde{\phi}_{b\mathbf{y}} >> = (H^{-1})_{a\mathbf{x},b\mathbf{y}} = (Q^{-1}\gamma_5)_{a\mathbf{x},b\mathbf{y}} \tag{5}$$

Note that separate pseudofermion fields are needed for each quark propagator as averages of products of (say) four *bosonic* pseudofermion fields will produce contractions with the wrong sign relative to the corresponding fermionic 4 quark amplitudes. The simulation of averages of the kind found in (3,4,5) can be readily accomplished by heat-bath updates, due to the simple Gaussian dependence of the action on the fields. For either Wilson or clover-improved actions, the dependence of the pseudofermion weight on the pseudofermion field at a specific lattice site $\mathbf{x}$ takes the form

$$e^{-S_{\mathrm{pf}}} \simeq e^{-\phi_{a\mathbf{x}}^{\dagger}A_{\mathbf{x}ab}\phi_{b\mathbf{x}}+4\kappa\mathrm{Re}(\phi_{a\mathbf{x}}^{*}v_{a\mathbf{x}})} \tag{6}$$

where $v_{a\mathbf{x}}$ is a complex spin-color vector assembled from the pseudofermion field at nearest and next-to-nearest sites, as well as appropriate gauge-link variables connecting to those sites. The 12x12 matrix A is a multiple of the identity (specifically $A = 1 + 16\kappa^2$) for Wilson actions, and a more complicated hermitian matrix assembled from clover gauge fields in the SW-improved case. In either case, the heat-bath update of $\phi_{\mathbf{x}}$ is readily managed by completing the square in (6). For the clover actions, the matrices $A_{\mathbf{x}ab}$ can be prediagonalized just once at the start of the simulation, and the resulting stored eigenvalues and eigenvectors used to quickly generate ϕ updates at each site according to the weight (6).

The pseudofermion method can be readily generalized to study the all-point overlap operator arising from an overlap action satisfying the Ginsparg-Wilson condition

[5, 6]. Let H be the hermitian Wilson-Dirac operator with suitably chosen overlap mass. The all-point overlap operator for arbitrary bare quark mass is trivially computable once all matrix elements of the nonlocal operator $\epsilon(H) \equiv H \cdot (H^2)^{-\frac{1}{2}}$ are obtained. Using an optimal rational approximation [7], this nonlocal operator can be written

$$\epsilon(H) \simeq (a_0 + \sum_{m=1}^{N} a_m \frac{1}{H^2 + b_m})H \tag{7}$$

where a_m are real and the b_m are real positive. The number of pole terms N needed for a given level of uniform accuracy over the spectrum of H is related in a fairly straightforward way to the condition number of H, but typical studies of the overlap operator have used $10 < N < 100$. We shall return to this issue in Section 4, where we show that mode-shifting can be used to dramatically improve this condition number and reduce the number of poles needed. The needed all-point operator can clearly be obtained by an average of N pseudofermion fields, $\phi^{(m)}, m = 1, N$: we begin from the positive definite action

$$S_{\text{pf,overlap}} = \sum_{m=1}^{N} \phi^{(m)\dagger}(H^2 + b_m)\phi^{(m)} \tag{8}$$

and construct the desired combination of pole terms from a corresponding combination of pseudofermion fields, averaged relative to the weight (8):

$$\epsilon(H)_{a\mathbf{x},b\mathbf{y}} = << \sum_{m} a_m \phi_{a\mathbf{x}}^{(m)} \phi^{(\tilde{m})}{}_{b\mathbf{y}} >> + a_0 H_{a\mathbf{x},b\mathbf{y}} \tag{9}$$

The computation of all-point overlap propagators will require a simulation within a simulation (analogously to the situation for single source overlap propagators, where inversions within an outer conjugate gradient inversion are required, [7]).

6

3   Hadronic Correlators from All-Point Pseudofermion Quark Propagators

In general, the computation of multipoint hadronic correlators involving n quark propagators can be reduced to convolutions of n pseudofermion fields, rapidly computed by fast Fourier transform (FFT). In fact, using FFT we can easily construct a wide range of correlators involving both local and smeared operators. In this section we shall illustrate this by considering a number of examples of physical interest. We note here that it may be advisable to combine all-point with conventional fixed source (or sink) propagators (obtained, say, from a conjugate gradient inversion), as accurate results become increasingly difficult as the number of allpoint propagators used increases, due to the large condition number of H, as will become clear in subsequent sections. Furthermore, the projection methods described in Section 5 become increasingly essential in reducing the statistical errors of the pseudofermion average as the number of independent all-point propagators increase.

3.1   Local Two-point Correlators

The all-point propagators obtained by the pseudofermion technique can be used to construct the complete momentum-space dependence of 2-point correlators of scalar or pseudoscalar densities, or vector or axial-vector currents, while exploiting the full physical content of each gauge configuration. For example, we may be interested in the full 4-momentum transform

$$\Delta_{PS-PS}(q) \equiv \sum_{x,y} e^{iq \cdot (x-y)} \Delta(x,y)$$

7

of the 2-point pseudoscalar correlator $\Delta(x,y)$, given by

$$\Delta(x,y) \;=\; < 0|T\{\bar{\Psi}(x)\gamma_5\Psi(x)\,\bar{\Psi}(y)\gamma_5\Psi(y)\}|0 > \tag{10}$$

$$=\; -< \mathrm{tr}((\mathbf{Q}^{-1}\gamma_5)_{\mathbf{xy}}(\mathbf{Q}^{-1}\gamma_5)_{\mathbf{yx}}) > \tag{11}$$

$$=\; -<< \sum_{ab} \phi_{xa}(\phi^\dagger H)_{yb}\chi_{yb}(\chi^\dagger H)_{xa} >>$$

$$=\; -<< (\phi^\dagger H\chi)_{yy}(\chi^\dagger H\phi)_{xx} >>$$

$$=\; -<< (\tilde{\phi}\cdot\chi)_{yy}(\tilde{\chi}\cdot\phi)_{xx} >> \tag{12}$$

where (10) represents a conventional operator VEV, the single brackets in (11) refer to a functional average over gauge-fields, and the double brackets in (12) imply averages over gauge configurations as well as a pseudofermion average for each gauge configuration to determine the all-point propagators Q^{-1} in (11). The full momentum-space correlator thus becomes an easily evaluated fast Fourier transform of products of pseudofermion fields:

$$\Delta_{PS-PS}(q) = -<< \mathrm{FFT}(\tilde{\chi}\cdot\phi)(\mathrm{q})\mathrm{FFT}(\tilde{\phi}\cdot\chi)(-\mathrm{q}) >> \tag{13}$$

At this point, it may be of use to the reader to indicate the computational requirementsof these pseudofermion simulations (see [8] for more details). For a 6^4 lattice, a single heat-bath update of the two pseudofermion fields ϕ, χ requires 0.366 sec. on a 1.5 GHz Pentium-4 processor. The convolutions and FFT operations required to obtain the desired four-momentum field $\Delta_{PS-PS}(q)$ in (13) require an additional 0.024 sec. and are performed after every 2 heat-bath updates of ϕ, χ. Typically, a sufficiently accurate pseudofermion average for $\Delta_{PS-PS}(q)$ was obtained from 20000 measurements, corresponding to 2.1 Pentium-4 hrs. For 10^3x20 lattices, a heat-bath update costs 3.30 sec, a measurement of $\Delta(q^2)$ requires 0.43 sec. (again, performed

8

every 2 heat-bath steps), and final averages are taken from 7000 measurements, corresponding to 6.8 Pentium-4 hrs. For comparison, the evaluation of a conventional conjugate-gradient single-source propagator on a 10^3x20 lattice requires 1.2 Pentium-4 hrs.

3.2   Smeared Meson Propagators

In lattice QCD, hadron spectroscopy is usually studied using smeared hadron sources/sinks to optimize the ground-state signal in each hadronic channel. A typical multistate propagation amplitude from Euclidean time t_i to t_f might therefore involve evaluation of the matrix

$$\mathcal{M}_{\alpha\beta}(t_i, t_f) \equiv \tag{14}$$

$$\sum_{\vec{x}\vec{y}\vec{z}\vec{w}} f_\alpha(\vec{x}) f_\beta(\vec{y}) < 0|T\{\bar{\Psi}(\vec{z}+\vec{x}, t_i)\gamma_5 O_\alpha \Psi(\vec{z}, t_i)\bar{\Psi}(\vec{w}+\vec{y}, t_f)\gamma_5 O_\beta \Psi(\vec{w}, t_f)\}|0 >$$

where $f_\alpha(\vec{x})$ are a set of spatial smearing wavefunctions, $\Psi(\vec{x}, t)$ denotes the quark field at spatial (lattice) point $\vec{x}$ and time t, and O_α are the appropriate spin matrices for the desired hadronic channels. The sums over $\vec{z}, \vec{w}$ project the physical states onto zero-momentum. Of course, delta function choices for f_α allow us to use local sources or sinks. In terms of pseudofermion quark propagators

$$\begin{aligned}\mathcal{M}_{\alpha\beta}(t_i, t_f) &\equiv -\sum_{\vec{x}\vec{y}\vec{z}\vec{w}} f_\alpha(\vec{x}) f_\beta(\vec{y})\{<< \tilde{\phi}_{\vec{w}+\vec{y}, t_f} O_\beta \chi_{\vec{w}, t_f} \tilde{\chi}_{\vec{z}+\vec{x}, t_i} O_\alpha \phi_{\vec{z}, t_i} >> \\ &- N_f << \tilde{\phi}_{\vec{z}+\vec{x}, t_i} O_\alpha \phi_{\vec{z}, t_i} \tilde{\chi}_{\vec{w}+\vec{y}, t_f} O_\beta \chi_{\vec{w}, t_f} >>\}\end{aligned} \tag{15}$$

where the second line of (15) (N_f=number of flavors) is present only for isoscalar amplitudes where there is a nonvanishing loop-back ("hairpin") amplitude. The four-fold spatial sum in (15) can fortunately be reduced to operations linear in the spatial

9

volume V_s of the lattice via the magic of Fourier transforms. Define smeared pseudo-fermion fields

$$
\begin{aligned}
\hat{\phi}^{\alpha}_{\vec{x},t_i} &\equiv \frac{1}{V_s} \sum_{\vec{p}} e^{i\vec{p}\cdot\vec{x}} f_{\alpha}(-\vec{p}) \phi_{\vec{p},t_i} \\
\hat{\chi}^{\beta}_{\vec{y},t_f} &\equiv \frac{1}{V_s} \sum_{\vec{p}} e^{i\vec{p}\cdot\vec{y}} f_{\alpha}(-\vec{p}) \chi_{\vec{p},t_f}
\end{aligned}
$$

where $f_{\alpha}(\vec{p})$ is the Fourier transform smearing function and $\phi_{\vec{p},t}$ represents the spatially Fourier transformed (and time-sliced) pseudofermion field. Taking the isovector amplitude part of (15) for simplicity, one finds that this reduces to

$$
\mathcal{M}^{\text{isovec}}_{\alpha\beta}(t_i,t_f) = - << (\sum_{\vec{x}} \tilde{\chi}_{\vec{x},t_i} O_{\alpha} \hat{\phi}^{\alpha}_{\vec{x},t_i}) \cdot (\sum_{\vec{y}} \tilde{\phi}_{\vec{y},t_f} O_{\beta} \hat{\chi}^{\beta}_{\vec{y},t_f}) >> \tag{16}
$$

The isoscalar contribution, if present, is trivially obtained by interchanging the pseudofermion fields in an obvious way.

3.3   Three Point Functions - The Pion Form Factor

The computation of more complicated correlators, such as the 3-point functions needed to extract form factors, is greatly facilitated if we have all-point quark propagators at our disposal. A typical example is shown in Fig.1, where a smeared meson created at time t_0 propagates to time t_1, where spacelike momentum q is injected at spacetime point $(\vec{y}, t_1)$ by an electromagnetic current, followed by propagation of the final-state meson to time t_2, when it is removed by an appropriate smeared-sink operator.

The quark diagram displayed in Fig. 1 represents the connected contribution to
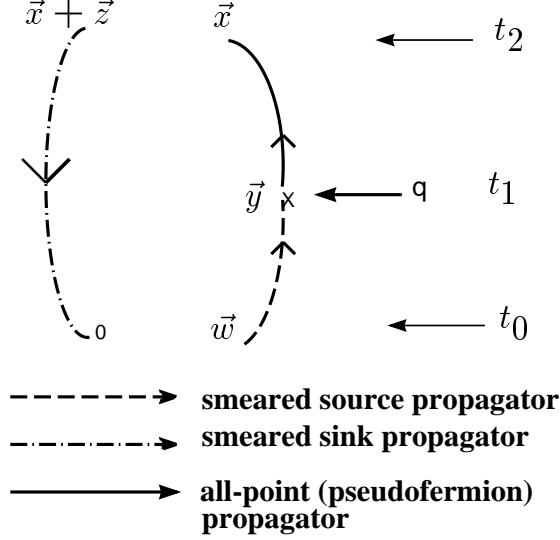
Figure 1: Quark flow diagram for computing pion form factor(connected part)

the following hadronic correlator:

$$J_{t_0 t_1 t_2}(\vec{q}) = \sum_{\vec{w}\vec{x}\vec{y}\vec{z}} e^{i\vec{q}\cdot(\vec{x}-\vec{y})} f^{\text{sm}}(\vec{z}) f^{\text{sm}}(\vec{w})$$

$$\cdot < \bar{\Psi}(\vec{z}+\vec{x},t_2)\gamma_5\Psi(\vec{x},t_2)\bar{\Psi}(\vec{y},t_1)\gamma_0\Psi(\vec{y},t_1)\bar{\Psi}(\vec{w},t_0)\gamma_5\Psi(0,t_0) > \qquad (17)$$

where in this case the same smearing function f^{sm} (optimized for a pion, say) is applied at both initial and final times. The complete momentum-dependence of this 3-point function can be obtained by using an all-point pseudofermion propagator for the quark propagator from $(\vec{y}, t_1)$ to $(\vec{x}, t_2)$. The quark propagators into the point sink at $(0, t_0)$ and from the smeared source point at $(\vec{w}, t_0)$ can be computed by conventional conjugate-gradient techniques. Again, by using Fourier transforms appropriately, the calculation of $J_{t_0 t_1 t_2}(\vec{q})$ can be reduced to operations at most linear in the spatial lattice volume. Finally, as for the case of smeared meson propagators discussed above, the disconnected contribution involving the contraction of $\Psi(\vec{y}, t_1)$

back to $\bar{\Psi}(\vec{y}, t_1)$ can be calculated with no extra effort, as the all-point propagator for just this case has been computed. In this case the pseudofermion field will appear in an average of the form $<< \tilde{\phi}_{\vec{y}t_1} \gamma_0 \gamma_5 \phi_{\vec{y}t_1} >>$.

4 Statistical Properties of Pseudofermion Propagators

In this section we shall describe the results of detailed studies of the statistical properties of pseudofermion propagators computed from the basic formulas (3). We first consider a case where only one all-point propagator is used in assembling the full hadronic amplitude- namely, the 3-point correlator $J(q)$ giving the pion formfactor discussed in Section 3.3. We shall see shortly that as a consequence of the typically high condition number of the hermitian Wilson-Dirac operator H, autocorrelations for low-momentum amplitudes become progressively longer as more all-point propagators are introduced into the calculation (in Section 5, we shall show how to fix this problem by mode-shifting). Here, we begin with an application where autocorrelations are relatively unproblematic.

For the pion form-factor calculation, we generated quenched configurations at β =5.9 on 12^3x24 lattices, and studied the resulting quark propagators at κ =0.1590 (with the Wilson action). The results described here were obtained by studying the simulation of the quantity $J(q)$ for a randomly chosen gauge configuration from this ensemble: examination of other configurations reveals that the behavior we describe is generic. From Eq(4) the (infinite ensemble) average pseudofermion action should therefore be S_{pf} =497664. From Fig.2 it is apparent that the equilibrium value for this quantity is reached rather quickly, after about 20 heat-bath sweeps through the lattice. An average of the value of 200 consecutive pseudofermion configurations after this gives for example S_{pf} =497599 with a standard deviation of $\simeq$650. Typically, we
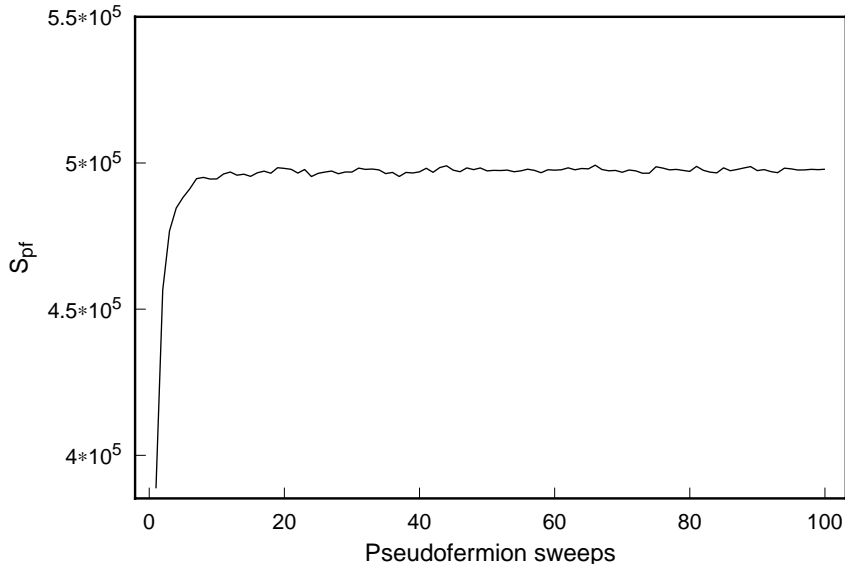
Figure 2: Equilibration of pseudofermion average on 12^3x24 lattices

have performed measurements using pseudofermion fields after 100 initial sweeps.

The decorrelation of hadronic amplitudes in the course of a MonteCarlo simulation of the pseudofermion propagator (3) is extremely sensitive to the particular momentum component being calculated. In particular, low momentum components have a large overlap with the smallest eigenmodes of H, which can have very small eigenvalues ($\simeq 10^{-3}$ is not uncommon). These low modes decorrelate only slowly in any local update of the action (2). This property becomes immediately apparent when we examine the momentum dependence of either the convergence of cumulative averages (Fig.3) of $J(q^2)$ (taking $t_2 - t_1 = t_1 - t_0$=3) or the autocorrelation function of the same quantity (Fig.4), as a function of number of pseudofermion heat-bath sweeps performed. The autocorrelation time (defined as the integral under the autocorrelation curve of Fig. 4) turns out to be about 13 for the zero-momentum mode
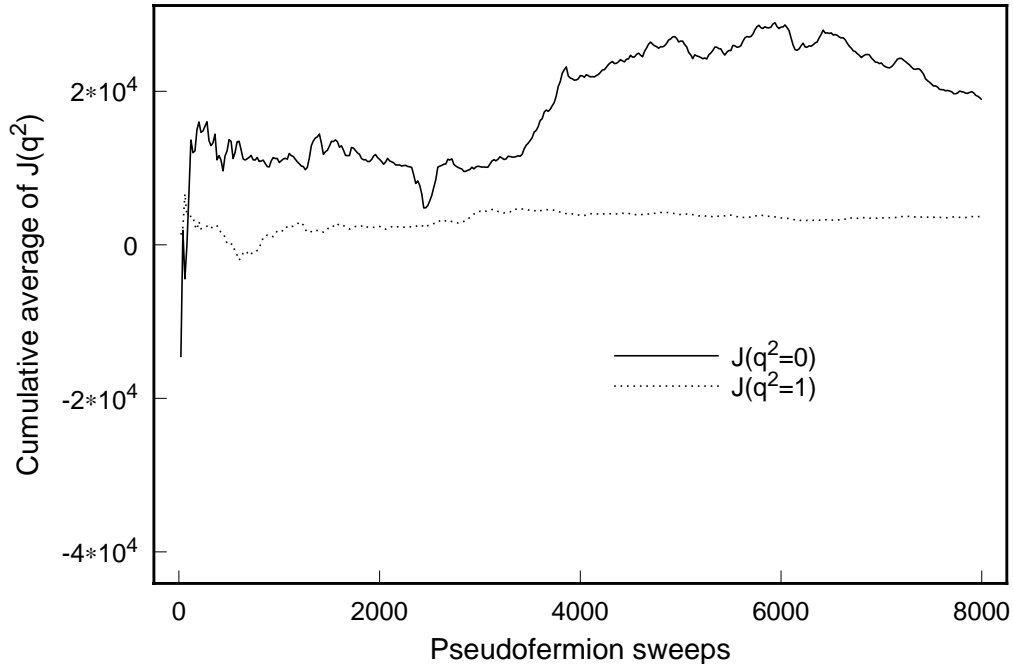
14

Figure 3: Cumulative averages for pion form-factor amplitude $J(q^2), q^2 = 0, 1$

and 7 for the $q^2 = 1$ (lattice units) mode: higher momenta (not shown here) yield autocorrelation times of order unity. In fact, the autocorrelation times for this correlator are fairly mild in comparison to the cases involving two all-point propagators discussed below: 8000 pseudofermion sweeps ($= \simeq 12$ hrs on a 1.5GHz Pentium 4) allow $J(q)$ to be extracted with error bars well below the intrinsic fluctuation of the correlator from one gauge configuration to the next (see Fig.5).

The critical slowing down seen in low eigenmodes becomes a more serious problem in situations where two separate all-point propagators are required to construct the desired correlator, as in the local two-point correlators discussed in Section 3.1. In this case the very large condition number of H^2 implies an *extremely* slow convergence for the zero-momentum component of the correlator. For example, from (11) we see
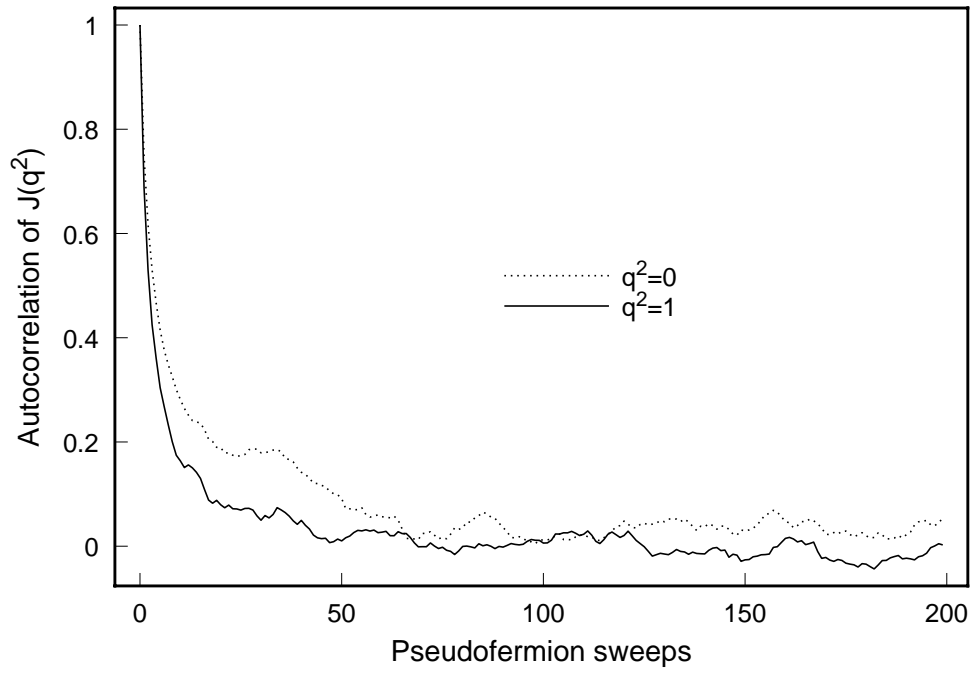
15

Figure 4: Autocorrelation function of pion form-factor amplitude $J(q^2), q^2 = 0, 1$

that the local pseudoscalar density correlator can be written, in momentum space

$$\Delta_{PS-PS}(q) = \sum_{x,y} e^{iq \cdot (x-y)} \text{Tr}((H_{xy}^{-1} H_{yx}^{-1})) \tag{18}$$

which becomes, for zero momentum

$$\Delta_{PS-PS}(0) = \text{Tr}(\frac{1}{H^2}) \tag{19}$$

As one not uncommonly encounters small eigenvalues of H, it is apparent that a few low eigenmodes can contribute disproportionately to this quantity. Moreover, these are exactly the modes that decorrelate most slowly in the pseudofermion simulation. To illustrate this, we have studied [8] hadronic 2-point correlators on an ensemble of unquenched configurations generated with the truncated determinant algorithm (TDA,[9]) on physically large coarse 6^4 lattices (lattice spacing $\simeq 0.4$ fm). Cumulative averages for $\Delta_{PS-PS}(q)$ for a range of values of q^2, for a typical gauge configuration in this ensemble, are shown in Fig. 5. The zero momentum mode is clearly not convergent even after 8000 pseudofermion sweeps, while even the smallest nonzero (lattice) momentum component shows much more rapid convergence. For the particular gauge configuration illustrated here, the lowest eigenvalue of H turns out to be 0.0024, which contributes 54% of the total zero-momentum value $\text{Tr}\frac{1}{H^2}$! The problem for this lowest mode can be seen (Fig. 6) in another guise in the autocorrelation curves for $\Delta_{PS-PS}(q^2), 0 \leq q^2 \leq 2$ (the autocorrelation time is $\simeq 1$ pseudofermion sweep for $q^2 > 2$ (lattice units) so these curves are not shown). Fortunately, the critical slowing down experienced in these pseudofermion simulations of all-point propagators appears only to infect the very lowest momentum components. We shall see in the next section that the problem can be eliminated for these components by mode-shifting a relatively small number of low eigenmodes of H. This
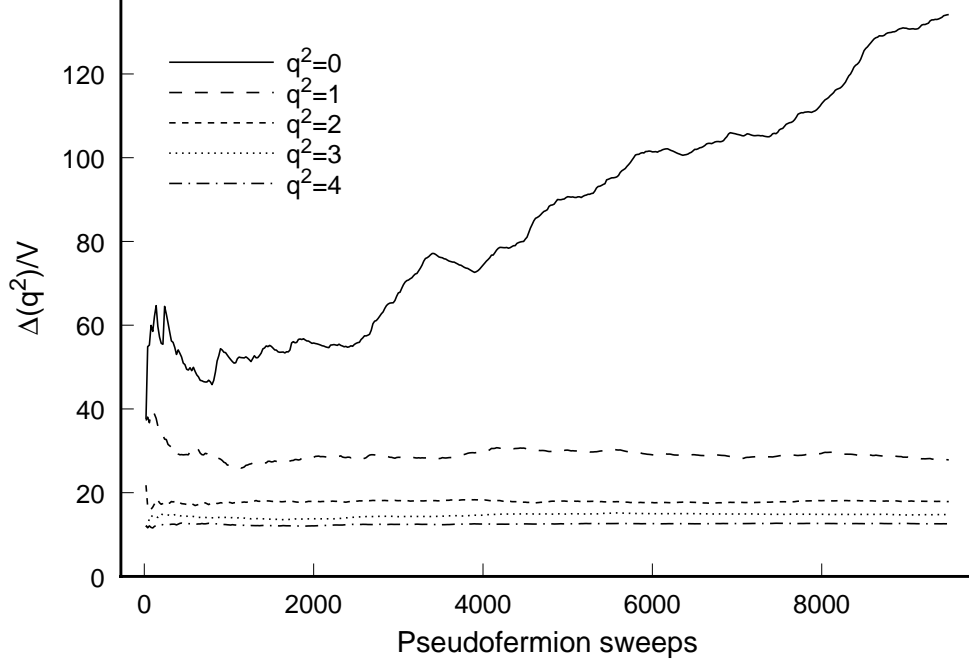
17

Figure 5: Cumulative averages of pseudoscalar density correlator $\Delta_{PS-PS}(q^2)$, $0 \le q^2 \le 4$

preconditioning substantially reduces autocorrelation times and allows us to extract reasonably accurate values even for the zero-momentum component of hadronic correlators. The extraction and separate treatment of low eigenmodes is also essential in calculating accurate all-point overlap operators.
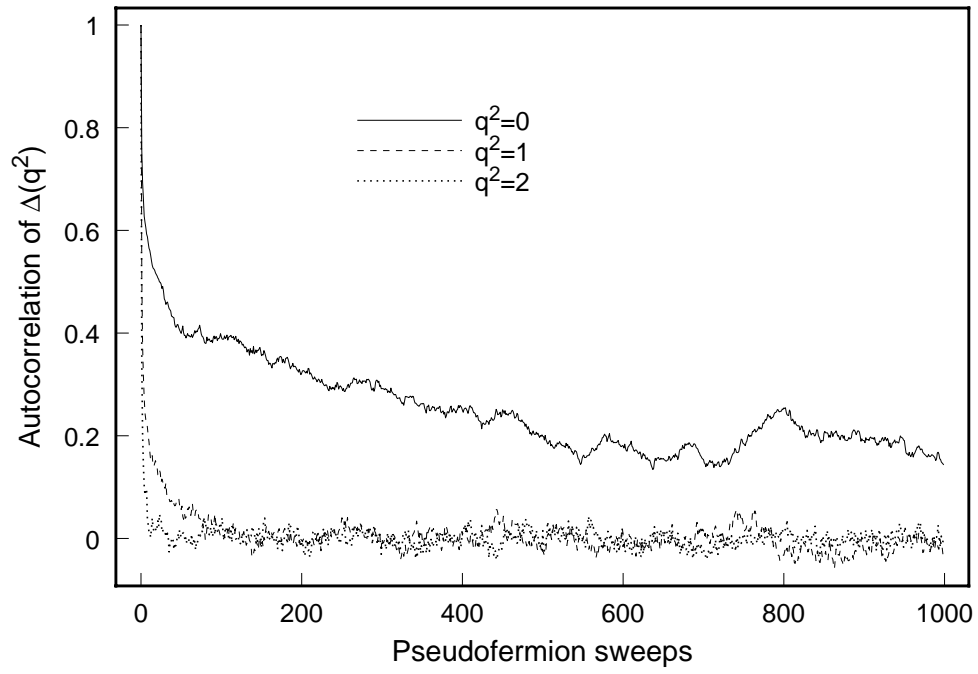
Figure 6: Autocorrelation curves of pseudoscalar density correlator $\Delta_{PS-PS}(q^2)$, $0 \leq$ $q^2 \leq 2$

5 Mode-Shifted Simulations of All-Point Propagators

The slow convergence of the lowest momentum modes discussed in the preceding section can be substantially accelerated by shifting the low eigenmodes of the Hermitian Wilson-Dirac operator H responsible for the critical slowing down. In the case of the two-point correlator (18), the relevant parameter is the condition number of H^2, which (for the ensemble of unquenched 6^4 lattices discussed in Section 4) can typically be reduced by two orders of magnitude by shifting the lowest 10 eigenmodes of H^2. More generally, define

$$H_s \equiv H + \sum_{i=1}^{N} \delta_i \mathbf{v}_i \mathbf{v}_{\mathbf{i}}^{\dagger} \tag{20}$$

where $\mathbf{v}_i$ are a complete orthonormal set of eigenmodes of H, $H\mathbf{v}_i = \lambda_i \mathbf{v}_i$, and the lowest N modes (in absolute value) are shifted:

$$\delta_i \equiv \lambda_i^{(s)} - \lambda_i \tag{21}$$

For simplicity we shall take $\lambda_i^{(s)} = \text{sign}(\lambda_i^{(s)})$ henceforth, although any value with magnitude of order unity will do. The extraction of low eigenmodes of H is computationally straightforward using implicitly restarted Arnoldi techniques [15]: each mode requires a few minutes on a Pentium-4 processor for the 6^4 lattices discussed here. Corresponding to the shifted operator H_s defined in (20) is a shifted pseudofermion action:

$$S_{\text{s,pf}} = \sum_{a\mathbf{x},b\mathbf{y}} \phi_{a\mathbf{x}}^{*} (H_s^2)_{a\mathbf{x},b\mathbf{y}} \phi_{b\mathbf{y}} \tag{22}$$

Once the relevant low eigenmodes $\mathbf{v_i}$ are known, the heat-bath update of the pseudofermion field ϕ can be performed by trivial modifications of the procedure outlined

in Section 2. The added computational load is not large: if $N=10$ modes are shifted, the time required for a pseudofermion update increases by about 20%. For the rest of this section, we shall use the double-bracket notation $<< .... >>$ introduced in Section 2 to indicate averages relative to the weight generated by the shifted action $S_{\text{s,pf}}$. Accordingly, the *unshifted* quark propagator is given by

$$H^{-1}_{a\mathbf{x},b\mathbf{y}} = << \phi_{a\mathbf{x}}\tilde{\phi}_{b\mathbf{y}} >> - \sum_{i=1}^{N} \Delta_i \mathbf{v}_{i,a\mathbf{x}}\tilde{\mathbf{v}}_{i,b\mathbf{y}} \tag{23}$$

where

$$\Delta_i \equiv 1 - \frac{1}{\lambda_i^2} \tag{24}$$

and the tilde notation on the right-hand-side of (23) still refers to the unshifted operator H, as in (5). The pseudoscalar correlator in (10-12) can therefore be written

$$\begin{aligned}
\Delta_{PS-PS}(q) &= \sum_{a\mathbf{x},b\mathbf{y}} e^{iq\cdot(\mathbf{x}-\mathbf{y})} H^{-1}_{a\mathbf{x},b\mathbf{y}} H^{-1}_{b\mathbf{y},a\mathbf{x}} \\
&= \sum_{\mathbf{x},\mathbf{y}} e^{iq\cdot(\mathbf{x}-\mathbf{y})} \quad \{ \quad << (\tilde{\phi}\cdot\chi)_{\mathbf{y}}(\tilde{\chi}\cdot\phi)_{\mathbf{x}} - \sum_i \Delta_i((\tilde{\chi}\cdot\mathbf{v}_i)_{\mathbf{x}}(\tilde{\mathbf{v}}_i\cdot\chi)_{\mathbf{y}} + (\tilde{\mathbf{v}}_i\cdot\phi)_{\mathbf{x}}(\tilde{\phi}\cdot\mathbf{v}_i)_{\mathbf{y}}) >> \\
&\quad + \sum_{i,j} \Delta_i\Delta_j(\tilde{\mathbf{v}}_j\cdot\mathbf{v}_i)_{\mathbf{x}}(\tilde{\mathbf{v}}_i\cdot\mathbf{v}_j)_{\mathbf{y}} \}
\end{aligned} \tag{25}$$

The term involving a double sum $\sum_{i,j}$ over shifted modes in (25) does not involve pseudofermion fields and is therefore calculated just once. We see that the usual result (12) has to be supplemented by an average of overlaps of the two pseudofermion fields with the shifted eigenmodes. Again, this is computationally perfectly manageable.

The dramatic effect of shifting even a few low eigenmodes on the convergence of correlators built from pseudofermion averages is illustrated in Figs. 7,8,9,10. As expected, the worst behavior is found in the zero momentum mode, where the unshifted averages (Fig. 7) are still 60% below the correct answer after 50,000 pseudofermion sweeps, while only 10,000 sweeps already give a reasonably good result after the 10
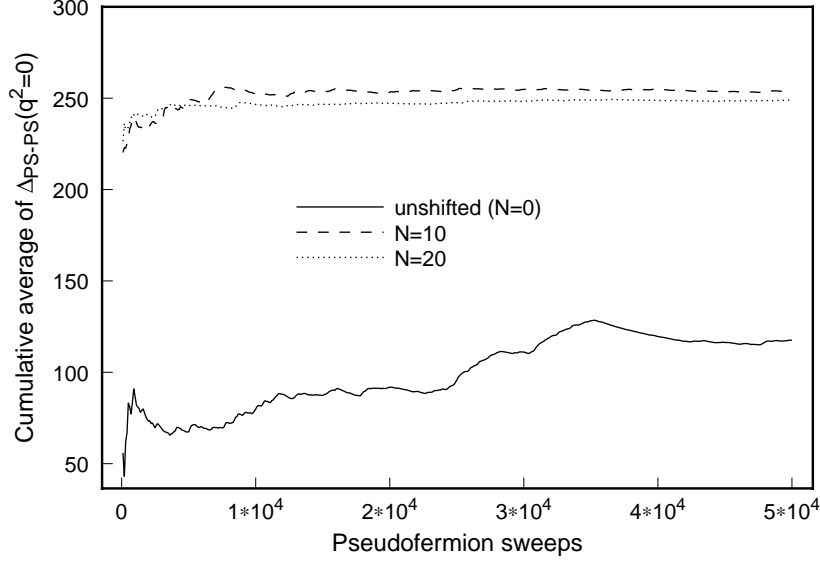
21

Figure 7: Cumulative average of zero-momentum pseudoscalar correlator

lowest modes are shifted. The autocorrelation curves for the zero-momentum component tell the same story (Fig. 8): the autocorrelation time is about 140 sweeps for the unshifted simulation, dropping to 11 (5) sweeps after shifting 10 (resp. 20) modes. The overall situation is much better for the lowest non-zero momentum mode, $q^2 = 1$, as shown in Figs. 9,10. Here the autocorrelation times are roughly 8,3,2 sweeps for simulations with 0,10 and 20 shifted modes respectively, and the cumulative averages reflect a correspondingly higher stability. The numerical evidence from these simulations clearly suggests that mode-shifting with N=10 modes, for the ensemble of 6^4 TDA lattices considered here, is perfectly adequate for obtaining accurate results at all momenta.

The calculation of an all-point overlap operator using (7) can be greatly facilitated by mode-shifting. The number N of poles needed in the optimal rational approxi-
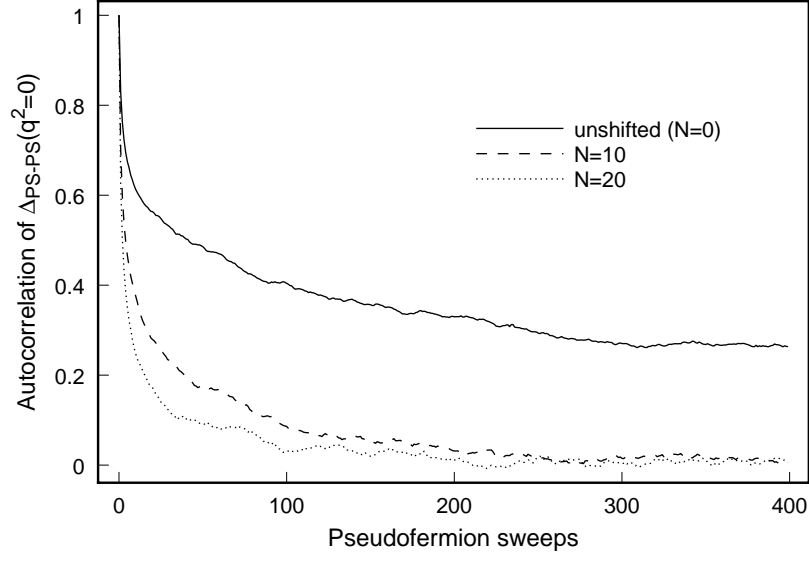
22

Figure 8: Autocorrelation curve for zero-momentum pseudoscalar correlator
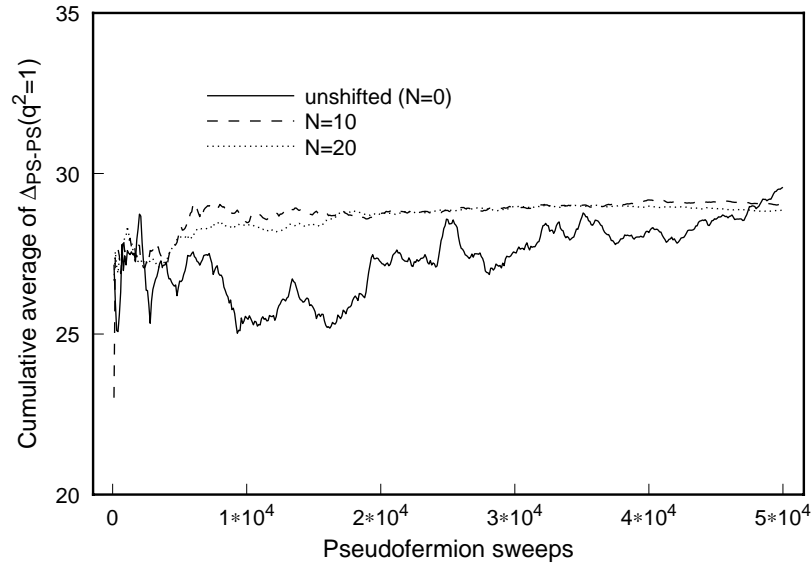

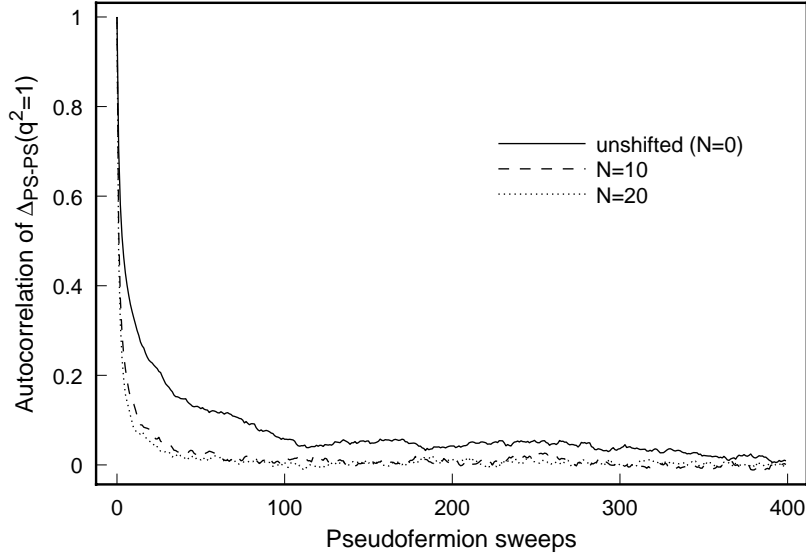Figure 9: Cumulative average for unit-momentum pseudoscalar correlator

Figure 10: Autocorrelation curve for unit-momentum pseudoscalar correlator

mation to achieve a desired uniform accuracy for $\epsilon(H)$ over the full spectrum of H is directly related to the condition number (ratio of highest to lowest eigenvalues) of H. On the other hand, provided the mode shifting preserves the algebraic sign of the shifted eigenvalues $(\mathrm{sign}(\lambda_i^{(s)})=\mathrm{sign}(\lambda_i))$, one clearly has $\epsilon(H_s) = \epsilon(H)$. Accordingly, the condition number of H can be drastically reduced by computing the overlap pseudofermion operator using (8) with H replaced with H_s as the pseudofermion action: the required code is identical to that used in the mode-shifted calculations of conventional Wilson propagators described above.

6 Acknowledgements

References

[1] G. M. de Divitiis, R. Frezzotti, M. Masetti and R. Petronzio, Phys. Lett. B **382**, 393 (1996).

[2] C. Michael and J. Peisa [UKQCD Collaboration], Phys. Rev. D **58**, 034506 (1998); Nucl. Phys. Proc. Suppl. **63**, 338 (1998); Nucl. Phys. Proc. Suppl. **60A**, 55 (1998).

[3] For a recent discussion, see K. Jansen and C. Liu, Nucl. Phys. B453 (1995) 375.

[4] M. Luescher, Nucl. Phys. **B418** (1994) 637.

[5] P.H. Ginsparg and K.H. Wilson, Phys.Rev. D25 (1982) 2649.

[6] R. Narayanan and H. Neuberger, Nucl. Phys. B443 (1995) 305.

[7] R. Edwards et al, Nucl. Phys. B540 (1999) 457.

[8] A. Duncan, S. Pernice and J. Yoo, "Matching Current Correlators in Lattice QCD to Chiral Perturbation Theory", in preparation.

[9] A. Duncan, E. Eichten and H. Thacker, Phys. Rev. D59 (1998) 014505.

[10] A. Duncan, E. Eichten and J. Yoo, "Hadronic Correlators from All-point Quark Propagators", (talk of A. Duncan at Lattice 2001, Berlin, Germany, Aug. 2001).

[11] A. Duncan, E. Eichten and H. Thacker, Phys. Rev. D63 (2001) 111501.

[12] M. Alford, W. Dimm, G.P. Lepage, G. Hockney and P.B. Mackenzie, Phys. Lett. B361 (1995) 87.

[13] H. Leutwyler and A. Smilga, Phys. Rev. D 46(1992)5607.

[14] Talk of E. Eichten, Lattice2001, Berlin, Germany Aug. 19-24,2001.

[15] For the ARPACK library, see www.caam.rice.edu/software/ARPACK.